CHANSON, H., and DOCHERTY, N.J. (2012). "Turbulent Velocity Measurements in Open Channel Bores." *European Journal of Mechanics B/Fluids*, Vol. 32, pp. 52-58 (DOI 10.1016/j.euromechflu.2011.10.001) (ISSN 0997-7546).

TURBULENT VELOCITY MEASUREMENTS IN OPEN CHANNEL BORES

by Hubert Chanson ([1]) and Nicholas J. Docherty ([1])

([1]) School of Civil Engineering, The University of Queensland, Brisbane QLD 4072, Australia.

Corresponding author:
Hubert Chanson, Professor
School of Civil Engineering, The University of Queensland
Brisbane QLD 4072, Australia
Fax: (61 7) 33 65 45 99 Email: h.chanson@uq.edu.au

Abstract:
In an open channel, a sudden rise in free-surface elevation is associated with the development of a bore. The bore front is a hydrodynamic shock with a sharp discontinuity in terms of water depth and velocity field. In this study, some turbulent velocity measurements were conducted in breaking bores. The unsteady turbulent properties were analysed using three methods: an ensemble-average (EA) technique based upon twenty repeated experiments, a variable interval time average (VITA) method based upon a single experiment, and the variable interval time average (VITA) method averaged over twenty experimental runs. The instantaneous free-surface and velocity measurements showed a marked effect of the bore front passage. The longitudinal velocity components were always characterised by a rapid flow deceleration at all vertical elevations, and some large fluctuations of all velocity components were recorded beneath the surge. The EA and VITA methods showed some comparable long-term trends superposed to some rapid turbulent fluctuations, as well as close results in terms of the turbulent Reynolds stress components. The variable interval time averaged (VITA) data based upon a single run presented some differences with the ensemble-averaged (EA) median results, but all methods exhibited comparable long-term trends superposed to rapid turbulent fluctuations.

Keywords: Breaking bores, Open channel flows, Turbulent velocity measurements, Acoustic Doppler velocimetry, Ensemble-average, Variable interval time average, Turbulent shear stresses, Tidal bores, Unsteady turbulence.

1. INTRODUCTION

A positive surge, also called a hydraulic jump in translation, is generated by the sudden rise in free-surface elevation in an open channel (Henderson 1966, Liggett 1994, Chanson 2009). In an estuary with macro-tidal conditions, the rapid water level rise at the river mouth might form such a positive surge, called a tidal bore, during the early flood tide (Rayleigh 1908, Peregrine 1966, Chanson 2011). Figure 1 presents an example of tidal bore in the Bay of Mont Saint Michel (France). At the bore front, there is discontinuity in terms of the water depth and velocity and pressure fields. The bore is a hydrodynamic shock (Lighthill 1978). Some unsteady velocity measurements, performed using PIV and ADV techniques by Hornung et al. (1995) and Koch and Chanson (2009), highlighted some large velocity fluctuations during the bore passage.

CHANSON, H., and DOCHERTY, N.J. (2012). "Turbulent Velocity Measurements in Open Channel Bores." *European Journal of Mechanics B/Fluids*, Vol. 32, pp. 52-58 (DOI 10.1016/j.euromechflu.2011.10.001) (ISSN 0997-7546).

Field measurements in tidal bores are rare despite their relevance. Several studies experienced some damage to the scientific equipments, including in the Rio Mearim (Brazil), in the Daly River (Australia), in the Dee River (UK), and in the Sélune River (France) (Kjerfve and Ferreira 1993, Wolanski et al. 2004, Simpson et al. 2004, Mouaze et al. 2010). The field works showed further some massive sedimentary processes in Alaska, China and France for example (Chen et al. 1990, Tessier and Terwindt 1994, Greb and Archer 2007). For example, the author saw the Sélune River in Bay of Mont Saint Michel (Fig. 1) cutting a new river channel during a single flood tide event on 31 August 2008, and other channel incision events were observed (Tessier, B. (2008), Person. Comm.). In the natural system, the channel bathymmetry does change rapidly and it is a challenge to characterise the flow turbulence based upon an unique experimental data set.

In this study, the turbulence properties of bores in open channels were investigated physically under controlled flow conditions. The free-surface fluctuations and turbulent velocity components were measured simultaneously, and the experiments were repeated 20 times with two different configurations. The turbulence properties of the breaking bore were analysed using three methods. The results were compared and discussed in the context of a hydrodynamic shock propagating in an open channel.

2. EXPERIMENTAL APPARATUS AND PROCEDURES

The experiments were performed in a 12 m long, 0.5 m wide tilting flume (Fig. 2). The channel was made of smooth PVC bed and glass walls and the water was supplied by a constant head tank. A fast-closing gate was located next to the channel downstream end (x = 11.15 m) where x is the distance from the channel upstream end. The experiments were performed with two types of bed roughness (Table 1). Some experiments were performed with the smooth PVC bed. For other experiments, the invert was covered with a series of plywood sheets covered by natural blue granite gravels which were sieved between 4.75 mm and 6.70 mm, glued in resin and covered by a spray gloss surface finish (Fig. 2B). The hydraulic roughness of the fixed gravel bed was tested for a range of steady flow conditions; the equivalent Darcy-Weisbach friction factor of the fixed gravel bed ranged from f = 0.031 to 0.045. The results were basically independent of Reynolds number and relative roughness, yielding on average f = 0.036 that corresponded to an equivalent sand roughness height k_s = 3.4 mm which was comparable to the typical gravel size d_s = 5.7 mm.

The steady flow rate was measured with two orifice meters that were calibrated on site with a volume per time technique. The percentage of error was expected to be less than 2%. In steady flows, the water depths were measured using rail mounted pointer gauges. The unsteady water depths were recorded using several acoustic displacement meters Microsonic™ Mic+25/IU/TC, with a response time of less than 50 ms and an accuracy of 0.2 mm. The acoustic displacement meters were calibrated against the pointer gauges in steady flows.

The turbulent velocity measurements were performed with an acoustic Doppler velocimeter (ADV) Nortek™ Vectrino+ (Serial No. VNO 0436) equipped with a side-looking head (Fig. 2B). The velocimeter head is seen above the free-surface in Figure 2B. During the experiments, the velocity range was 1.0 m/s, and the data accuracy was 0.01 m/s. The translation of the ADV probe in the vertical direction was controlled by a fine adjustment travelling mechanism connected to a Mitutoyo™ digimatic scale unit. The error on the vertical position of the probe was $\Delta z < 0.025$ mm where z is the vertical elevation. The accuracy on the longitudinal position was estimated as $\Delta x < +/- 2$ mm. The accuracy on the transverse position of the probe was less than 1 mm. Herein all the measurements were taken on the channel centreline since some earlier works showed little transverse differences but close to the sidewall where the

acoustic Doppler velocimetry could be adversely affected by the sidewall proximity (Chanson et al. 2007, Koch and Chanson 2009).

Further information on the experimental apparatus was reported by Docherty and Chanson (2010).

2.1 Acoustic Doppler velocimetry data post processing

During some initial tests, the ADV signal outputs contained numerous errors, associated with low correlations and low signal to noise ratios, caused by some inadequate seeding of the tap water. Thereafter the channel was seeded with about 100 g of Clay Ceram for every hour of channel operation. The clay powder was introduced in the intake structure upstream of the channel test section and dispersed progressively with time. All reported experimental data were conducted with some seeding.

The post processing of ADV data was conducted using a similar method to Koch and Chanson (2009). To characterise the steady flow properties only, the ADV post processing included the removal of communication errors, the removal of average signal to noise ratio data less than 5 dB, the removal of average correlation values less than 60%, and the application of the phase-space thresholding technique to remove spurious spikes from the data set (Goring and Nikora 2002). The percentage of erroneous data was less than 15% in steady flows, but close to the bed ($z < 0.030$ m) where the percentage was less than 30%.

In unsteady flow conditions, the above post-processing technique was not applicable (e.g. Nikora 2004, *Person. Comm.*, Koch and Chanson 2009). The unsteady flow post-processing was limited to a removal of communication errors, and it is acknowledged that the vertical velocity component V_z data might be affected adversely by the bed proximity for $z < 0.030$ m.

2.2 Experimental flow conditions and bore generation

The experimental setup was selected to generate a range of bores with the same initial flow rate Q (Table 1). The dependant parameters were the bed roughness and the downstream gate opening after closure h. For each experimental run, the steady gradually-varied flow conditions were established for 5 minutes prior to the measurement start. The tidal bore was generated by the rapid partial closure of the downstream gate (Fig. 2A). The gate closure time was less than 0.15 s. After closure, the bore propagated upstream (Fig. 3) and each experiment was stopped before the bore front reached the channel upstream end. The initial flow conditions as well as the tidal bore generation were highly repeatable.

Two series of experiments were conducted (Table 1). The first series focused on the general flow patterns and free-surface properties recorded between $x = 4$ and 6 m. In the second series of experiments, some detailed velocity measurements were conducted at $x = 5$ m, and the ADV and displacement sensors were sampled simultaneously at 200 Hz and synchronised within 5 ms. The velocity measurements were performed with flow conditions that could be considered roughly as a 3:1 scale study of the breaking bore seen in Figure 1.

Some preliminary steady flow measurements showed that, at $x = 5$ m, the velocity profile was partially-developed. The relative boundary layer thickness δ/d_o was 0.47 and 0.64 for the smooth PVC bed and fixed gravel bed respectively, where δ is the boundary layer thickness and d_o is the initial flow depth at $x = 5$ m (Table 1, column 7).

CHANSON, H., and DOCHERTY, N.J. (2012). "Turbulent Velocity Measurements in Open Channel Bores." *European Journal of Mechanics B/Fluids*, Vol. 32, pp. 52-58 (DOI 10.1016/j.euromechflu.2011.10.001) (ISSN 0997-7546).

2.3 Turbulent velocity calculations

In a turbulent flow, the instantaneous velocity V is typically decomposed into an average component $\overline{V}$ and a turbulent fluctuation v such as V = $\overline{V}$ + v. In a steady turbulent flow, $\overline{V}$ is the time-average. In an unsteady flow, the long-term trend and the short-term turbulent fluctuations must be processed separately (Bradshaw 1971, Piquet 1999). A technique consists in the repetition of the same experiment for N times, and $\overline{V}$ is the ensemble-average (Bradshaw 1971, Michel et al. 1981). Other techniques may be based upon the phase averaging method of periodic flows (Stutz and Reboud 1997), or some decomposition of turbulent time or length scales (Trowbridge 1998, Shaw and Trowbridge 2001). Another technique separates the distinctive long-term trend from the short-term fluctuation frequencies, and the variable interval time average $\overline{V}$ (VITA) is a low-pass filtered component (Piquet 1999).

In the present study, a series of twenty instantaneous velocity records were repeated at three vertical elevations (z/d_o = 0.135, 0.434 and 0.733) in a manner such that the initial flow conditions were perfectly identical for each run, where z is the vertical elevation and d_o the initial flow depth. An ensemble-median of each instantaneous velocity component was produced for each vertical elevation. Similarly the variable interval time average (VITA) was calculated for each run. The VITA decomposition was based upon a band pass filter, with a cut-off frequency F_{cutoff} = 2 Hz derived from a sensitivity analysis (Docherty and Chanson 2010).

The overall results were used to compare the ensemble-median of the twenty runs, the median VITA value of the same twenty runs, and the VITA value of a single run (Table 2). The first two methods can only be applied to laboratory experiments performed under controlled flow conditions, while the third method might be applicable to field measurements. (Chanson et al. 2011, Mouaze et al. 2010)

3. BASIC OBSERVATIONS

3.1 Presentation

Some visual observations were conducted for a range of flow conditions listed in Table 1. Several patterns were observed to be functions of the bore Froude number defined as:

$$Fr = \frac{V_o + U}{\sqrt{g\,d_o}} \quad (1)$$

where V_o is the initial flow velocity positive downstream, g is the gravity acceleration and U is the surge front celerity positive upstream (Fig. 2A). The Froude number is defined herein in the system of co-ordinates in translation with the surge (Lighthill 1978, Liggett 1994). For a Froude number between unity and 1.5, the tidal bore was undular. That is, the tidal bore front was followed by a train of secondary, quasi-periodic waves called undulations (Fig. 3A). For larger Froude numbers (Fr > 1.5 to 1.6), a breaking bore was observed (Fig. 1 & 3B). It was characterised by a marked turbulent roller.

The undular bore had a smooth, quasi-two-dimensional free-surface profile for Fr < 1.2 to 1.4 for smooth PVC and rough gravel bed respectively (Fig. 3A). For 1.2 to 1.4 < Fr, some slight cross-waves (or shock waves) were observed, starting next to the sidewalls upstream of the first wave crest and intersecting next to the first crest on the channel centreline. For 1.3 to 1.45 < Fr < 1.5, some slight breaking appeared at the first wave crest next to the channel centreline, and the secondary waves became flatter. The size and strength of the roller increased with increasing Froude number until the roller occupied the entire channel width. At the largest bore Froude numbers (i.e. Fr > 1.5), the surge

had a marked roller, and appeared to be quasi-two-dimensional (Fig. 3B). There was no shock wave and the free-surface behind the roller was about horizontal although some large free-surface fluctuations were observed. Some air entrainment and intense turbulent mixing were seen in the bore roller.

Overall the present findings were comparable to earlier observations (Favre 1935, Treske 1994, Hornung et al.1995, Koch and Chanson 2009). In particular, the tidal bore flow patterns were independent of the bed roughness.

3.2 Ratio of conjugate depths

In a bore, the flow properties immediately upstream and downstream of the front must satisfy the continuity and momentum principles (Henderson 1966, Liggett 1994). Considering a bore travelling in a horizontal rectangular channel, the integral form of the equations of conservation of mass and momentum gives a series of relationships between the flow properties in front of and behind the bore front, such as:

$$\frac{d_{conj}}{d_o} = \frac{1}{2}\left(\sqrt{1+8\,Fr^2}-1\right) \quad (2)$$

where d is the water depth, the subscript o refers to the initial flow conditions and the subscript conj refers to the conjugate flow conditions, or new flow conditions, immediately after the bore passage (Fig. 2A). Equation (2) gives an expression of the ratio of conjugate depths as a function of the bore Froude number, and it is based the assumption of hydrostatic pressure distribution in front of and behind the bore front, while the friction losses are neglected.

For the present experiments, the data of the conjugate depth ratio d_{conj}/d_o are presented in Figure 4 and compared with Equation (2) and some prototype and laboratory data. The results highlighted a reasonable agreement between data and theory for both the smooth and rough bed configurations. The finding was consistent with a number of earlier observations (Henderson 1966, Montes 1998).

3.3 Instantaneous free-surface and velocity measurements

During the second series of experiments (Table 1), the free-surface and velocity components were sampled simultaneously on the channel centreline at x = 5 m, with the ADV sampling volume elevation ranging between 0.0058 < z < 0.09 m. On the fixed gravel bed, the vertical elevation z was measured above the top of the gravel bed using a semi-circular footing with a 25.1 cm^2 area. Figure 5 illustrates a typical data set in the form of the dimensionless time variations of instantaneous free-surface elevation and velocity components. Herein the instantaneous velocity components V_x, V_y and V_z were positive downstream, towards the left sidewall and upwards respectively.

On the smooth PVC bed, the surge was a breaking bore without residual free-surface undulations (Fig. 5). On the rough gravel bed, the surge had a marked roller followed by some small residual undulations, possibly linked with a small difference in bore Froude number. Both the free-surface data and the visual observations showed that the free-surface elevation rose first slowly, immediately prior to the roller (Fig. 5 & 6). Such gradual rise in free-surface ahead of the turbulent roller is sketched in Figure 6 and was previously reported by Hornung et al. (1995) and Koch and Chanson (2009). In Figure 6, the characteristic time t' corresponded to the free-surface discontinuity between the gentle free-surface rise and the turbulent roller. For t > t', the turbulent roller caused a sharp rise in the water elevation seen in Figures 3B and 5.

For both smooth and fixed gravel bed configurations, the longitudinal velocity data highlighted a rapid deceleration during the passage of the bore roller. As the bore front reached the sampling volume (x = 5 m), the water depth

increased first gradually with time for $t < t'$ (Fig. 5). The gradual rise in free surface was associated with a gradual longitudinal deceleration, and was followed by a sudden increase in the free surface elevation during the roller passage ($t > t'$). The sudden rise in water depth was associated with a sharp decrease in longitudinal velocity component seen in Figure 5. Further some transient negative longitudinal velocities V_x were observed next the invert (Fig. 5). This transient recirculation pattern was observed for $z/d_o < 0.31$ on the smooth PVC bed and $z/d_o < 0.56$ on the fixed gravel bed. Above, the longitudinal velocity component tended to remain positive for the entire bore passage record. The observations implied the existence of an unsteady recirculation pattern that was associated with some large turbulent stresses in the water column and would induce some major impact in a natural system in terms of sediment processes and particulate dispersion.

Most characteristic features were similar for both the smooth PVC and fixed gravel beds, although the bed roughness had a noticeable effect on the recirculation patterns in the flow.

5. UNSTEADY TURBULENCE PROPERTIES

5.1 Presentation

A series of twenty instantaneous free-surface and velocity records were repeated, and the data were synchronised in terms of the characteristic time t' (Fig. 6). Both the ensemble average (EA) and variable interval time average (VITA) techniques were applied. Figure 7 illustrates some typical difference in signal processing techniques. Figure 7 presents the median water depth d_{median} and median velocity component $(V_x)_{median}$, both ensemble-averaged (EA) over the 20 runs, the low-pass filtered velocity component, or VITA, of each run, and the median VITA value for the 20 runs. Figure 7A shows some longitudinal velocity data and Figure 7B some vertical velocity data. Figure 8 presents a further comparison between a longitudinal data set (Run 1), the VITA of the single run, and the median velocity component $(V_x)_{median}$. Some preliminary remarks may be derived from Figures 7 and 8. The median VITA value for the 20 runs and the ensemble averaged median data yielded close results in terms of all turbulent velocity components (Fig. 7). The VITA data based upon a single run provided the general trends despite some difference with the EA results (Fig. 8).

Overall both the ensemble-averaged (EA) and VITA data showed some seminal features of the breaking bores: (a) a rapid flow deceleration during the passage of the tidal bore roller above the sampling volume, (b) some negative longitudinal velocity component next to the bed highlighting some transient recirculation "bubble", and (c) some positive vertical velocity component beneath the roller. The latter was believed to be closely linked with the streamline curvature immediately prior to the bore roller ($t < t'$) and possibly during the roller propagation ($t' < t$). The experimental results showed further that the passage of the roller was always associated in some large free-surface fluctuations, associated with some large velocity fluctuations and some transient upward flow motion ($V_z > 0$).

The experimental results indicated that the ensemble-average (EA) median data were very close to the median VITA value for the 20 runs (Fig. 7 & 8). The finding was interesting practically since the ensemble-averaging method required less processing. The results highlighted however some differences: i.e., the time-variations of the VITA data for each individual run presented some scatter compared to the ensemble-averaged median value (Fig. 7 & 8). However all the techniques provided some comparable long-term trends superposed to rapid turbulent fluctuations of the turbulent velocity components. Lastly note the scatter of the ensemble-averaged data around the long-term tend. It is acknowledged that the number of experimental repeats (20 herein) was small.

5.2 Turbulent Reynolds stresses in breaking tidal bores

The Reynolds stress tensor is a transport effect resulting from turbulent motion induced by velocity fluctuations with its subsequent increase of momentum exchange and of mixing. Herein the instantaneous turbulent stresses were calculated using the ensemble-averaging (EA) and variable interval time averaging (VITA) techniques for the experimental flow conditions summarised in Table 1. Some typical results are presented in Figure 9. In Figure 9, the median Reynolds stress tensor components were calculated using either the ensemble-averaging (EA) and variable interval time averaging (VITA) methods (median value of 20 runs).

The turbulent stress results showed a number of interesting features. The Reynolds stress data suggested that the passage of breaking tidal bores was associated with large and rapid fluctuations of all the turbulent stresses at all vertical elevations. That is, the magnitude of the Reynolds stress tensor components was significantly larger than prior to the bore passage. For example, on the smooth PVC bed (Fig. 9A), the normal stress $\rho \times v_x^2$ increased from 0.6 Pa on average prior to the bore to 2.5 Pa on average beneath the breaking bore; similarly, on fixed gravel bed (Fig. 9C), $\rho \times v_x^2$ increased from 0.8 Pa on average prior to the bore to 4 Pa on average below the bore. The findings were observed for all Reynolds stress components. The result was consistent with the observations of Koch and Chanson (2009), but that study deduced the turbulent stresses from a VITA analysis performed on a single experiment. Koch and Chanson did not present any ensemble-averaged nor VITA median data.

Further the three processing techniques yielded similar results in terms of the Reynolds stresses. For example, both the ensemble-averaging and variable interval time averaging techniques yielded comparable results in terms of v_x^2 and $v_x v_y$ (Fig. 9).

6. CONCLUSION

In a highly unsteady flow, such as a shock, the turbulence measurements technique must be adapted, and this is detailed herein for positive surges and bores in an open channel. The experimental results demonstrated that the propagation of a breaking bore induced some substantial turbulent mixing. The passage of the bore front was associated with some large water depth fluctuations. Both the instantaneous and ensemble-averaged turbulent velocity data highlighted some basic features of the flow field in tidal bores. Namely a strong flow deceleration was observed at all elevations during the breaking bore passage. Close to the bed, the longitudinal velocity component became negative immediately after the roller passage implying the existence of a transient recirculation "bubble". The height and duration of the transient was a function of the bed roughness, with a longer, higher recirculation region above the fixed gravel bed. The vertical velocity data presented some positive, upward motion during the bore passage with increasing maximum vertical velocity with increasing distance from the bed, and it was believed to be linked with some streamline curvature. The transverse velocity data presented some large fluctuations with non-zero ensemble-average after the roller passage that highlighted some intense secondary motion advected behind the bore front.

A comparison between three processing techniques was developed (Table 2). The experimental findings highlighted a number of key features:

(a) Both the ensemble-average (EA) performed over 20 runs and ensemble-median of 20 variable interval time averages (VITA) showed some comparable long-term trends superposed to some rapid turbulent fluctuations. The result is valuable indicating that the method with the least processing (EA technique) was suitable in laboratory under controlled flow conditions.

CHANSON, H., and DOCHERTY, N.J. (2012). "Turbulent Velocity Measurements in Open Channel Bores." *European Journal of Mechanics B/Fluids*, Vol. 32, pp. 52-58 (DOI 10.1016/j.euromechflu.2011.10.001) (ISSN 0997-7546).

(b) The VITA data based upon a single run presented some differences with the EA median results in terms of all velocity components.

(c) The turbulent stress data showed comparable results with both EA and VITA techniques. The passage of the breaking bore was associated with large and rapid fluctuations of all turbulent stress components at each vertical elevation.

(d) All the techniques provided some comparable long-term trends superposed to rapid turbulent fluctuations of the turbulent velocity components.

Overall the study highlighted the intense turbulence and turbulent mixing during the passage of breaking bores and surges in open channels. The findings suggested further that the VITA for a single run gave the general trends and basic flow features; hence it may be a suitable technique for field measurements in tidal bores propagating in natural channels with movable boundaries and changing bathymetry between tides.

8. ACKNOWLEDGMENTS

The authors acknowledge the technical assistance of Graham Illidge and Clive Booth (The University of Queensland). The authors thank further Prof. Laurent David (University of Poitiers, France), Dr David Reungoat (University of Bordeaux, France) and Prof. C.J. Apelt (University of Queensland, Australia) for their helpful advice.

9. REFERENCES

Benet, F., and Cunge, J.A. (1971). "Analysis of Experiments on Secondary Undulations caused by Surge Waves in Trapezoidal Channels." *Jl of Hyd. Res.*, IAHR, Vol. 9, No. 1, pp. 11-33.

Bradshaw, P. (1971). "An Introduction to Turbulence and its Measurement." *Pergamon Press*, Oxford, UK, The Commonwealth and International Library of Science and technology Engineering and Liberal Studies, Thermodynamics and Fluid Mechanics Division, 218 pages.

Chanson, H. (2009). "Current Knowledge In Hydraulic Jumps And Related Phenomena. A Survey of Experimental Results." *European Journal of Mechanics B/Fluids*, Vol. 28, No. 2, pp. 191-210 (DOI: 10.1016/j.euromechflu.2008.06.004).

Chanson, H. (2011). "Current Knowledge in Tidal bores and their Environmental, Ecological and Cultural Impacts." Environmental Fluid Mechanics, Vol. 11, No. 1, pp. 77-98 (DOI: 10.1007/s10652-009-9160-5).

Chanson, H., Trevethan, M., and Koch, C. (2007). "Turbulence Measurements with Acoustic Doppler Velocimeters." *Journal of Hydraulic Engineering*, ASCE, Vol. 133, No. 11, pp. 1283-1286 (DOI: 10.1061/(ASCE)0733-9429(2005)131:12(1062)).

Chanson, H., Reungoat, D., Simon, B., and Lubin, P. (2011). "High-Frequency Turbulence and Suspended Sediment Concentration Measurements in the Garonne River Tidal Bore." *Estuarine Coastal and Shelf Science* (DOI 10.1016/j.ecss.2011.09.012) (Online First).

Chen, J., Liu, C., Zhang, C., and Walker, H.J. (1990). "Geomorphological Development and Sedimentation in Qiantang Estuary and Hangzhou Bay." *Jl of Coastal Res.*, Vol. 6, No. 3, pp. 559-572.

Docherty, N.J., and Chanson, H. (2010). "Characterisation of Unsteady Turbulence in Breaking Tidal Bores including the Effects of Bed Roughness." *Hydraulic Model Report No. CH76/10*, School of Civil Engineering, The University of Queensland, Brisbane, Australia, 112 pages.

CHANSON, H., and DOCHERTY, N.J. (2012). "Turbulent Velocity Measurements in Open Channel Bores." *European Journal of Mechanics B/Fluids*, Vol. 32, pp. 52-58 (DOI 10.1016/j.euromechflu.2011.10.001) (ISSN 0997-7546).

Favre, H. (1935). "Etude Théorique et Expérimentale des Ondes de Translation dans les Canaux Découverts." ('Theoretical and Experimental Study of Travelling Surges in Open Channels.') *Dunod*, Paris, France (in French).

Garcia, C.M., and Garcia, M.H. (2006). "Characterization of Flow Turbulence in Large-Scale Bubble-Plume Experiments." *Experiments in Fluids*, Vol. 41, No. 1, pp. 91-101.

Goring, D.G., and Nikora, V.I. (2002). "Despiking Acoustic Doppler Velocimeter Data." *Jl of Hyd. Engrg.*, ASCE, Vol. 128, No. 1, pp. 117-126. Discussion: Vol. 129, No. 6, pp. 484-489.

Greb, S.F., and Archer, A.W. (2007). "Soft-Sediment Deformation Produced by Tides in a Meizoseismic Area, Turnagain Arm, Alaska." *Geology*, Vol. 35, No. 5, pp. 435-438.

Henderson, F.M. (1966). "Open Channel Flow." *MacMillan Company*, New York, USA.

Hornung, H.G., Willert, C., and Turner, S. (1995). "The Flow Field Downstream of a Hydraulic Jump." *Jl of Fluid Mech.*, Vol. 287, pp. 299-316.

Kjerfve, B., and Ferreira, H.O. (1993). "Tidal Bores: First Ever Measurements." *Ciência e Cultura (Jl of the Brazilian Assoc. for the Advancement of Science)*, Vol. 45, No. 2, March/April, pp. 135-138.

Koch, C., and Chanson, H. (2009). "Turbulence Measurements in Positive Surges and Bores." *Journal of Hydraulic Research*, IAHR, Vol. 47, No. 1, pp. 29-40 (DOI: 10.3826/jhr.2009.2954).

Liggett, J.A. (1994). "Fluid Mechanics." *McGraw-Hill*, New York, USA.

Lighthill, J. (1978). "Waves in Fluids." *Cambridge University Press*, Cambridge, UK, 504 pages.

Michel, R., Cousteix, J., and Houdeville, R. (1981). "Unsteady Turbulent Shear Flows." *Springer Verlag*, Berlin, Germany, 424 pages.

Montes, J.S. (1998). "Hydraulics of Open Channel Flow." *ASCE Press*, New-York, USA, 697 pages.

Mouze, D., Chanson, H., and Simon, B. (2010). "Field Measurements in the Tidal Bore of the Sélune River in the Bay of Mont Saint Michel (September 2010)." Hydraulic Model Report No. CH81/10, School of Civil Engineering, The University of Queensland, Brisbane, Australia, 72 pages.

Navarre, P. (1995). "Aspects Physiques du Caracteres Ondulatoire du Macaret en Dordogne." ('Physical Features of the Undulations of the Dordogne River Tidal Bore.') *D.E.A. thesis*, Univ. of Bordeaux, France, 72 pages (in French).

Peregrine, D.H. (1966). "Calculations of the Development of an Undular Bore." *Jl. Fluid Mech.*, Vol 25, pp.321-330.

Piquet, J. (1999). "Turbulent Flows. Models and Physics." *Springer*, Berlin, Germany, 761 pages.

Rayleigh, Lord (1908). "Note on Tidal Bores." *Proc. Royal Soc. of London, Series A containing Papers of a Mathematical and Physical Character*, Vol. 81, No. 541, pp. 448-449.

Shaw, W.J., and Trowbridge, J.H. (2001). "The Direct Estimation of Near-Bottom Turbulent Fluxes in the Presence of Energetic Wave Motions." *Jl of Atmospheric and Oceanic Tech.*, Vol. 18, pp. 1540-1557.

Simpson, J.H., Fisher, N.R., and Wiles, P. (2004). "Reynolds Stress and TKE Production in an Estuary with a Tidal Bore." *Estuarine, Coastal and Shelf Science*, Vol. 60, No. 4, pp. 619-627.

Stutz, B., and Reboud, J.L. (1997). "Experiments in Unsteady Cavitation." *Experiments in Fluids*, Vol. 22, pp. 191-198.

Tessier, B., and Terwindt, J.H.J. (1994). "An Example of Soft-Sediment Deformations in an intertidal Environment - The Effect of a Tidal Bore". *Comptes-Rendus de l'Académie des Sciences*, Série II, Vol. 319, No. 2, Part 2, pp. 217-233 (in French).

Treske, A. (1994). "Undular Bores (Favre-Waves) in Open Channels - Experimental Studies." *Jl of Hyd. Res.*, IAHR, Vol. 32, No. 3, pp. 355-370. Discussion: Vol. 33, No. 3, pp. 274-278.

CHANSON, H., and DOCHERTY, N.J. (2012). "Turbulent Velocity Measurements in Open Channel Bores." *European Journal of Mechanics B/Fluids*, Vol. 32, pp. 52-58 (DOI 10.1016/j.euromechflu.2011.10.001) (ISSN 0997-7546).

Trowbridge, J.H. (1998). "On a Technique for Measurement of Turbulent Shear Stress in the Presence of Surface Waves." *Jl of Atmospheric and Oceanic Tech.*, Vol. 15, pp. 290-298.

Wolanski, E., Williams, D., Spagnol, S., and Chanson, H. (2004). "Undular Tidal Bore Dynamics in the Daly Estuary, Northern Australia." *Estuarine, Coastal and Shelf Science*, Vol. 60, No. 4, pp. 629-636 (DOI: 10.1016/j.ecss.2004.03.001).

CHANSON, H., and DOCHERTY, N.J. (2012). "Turbulent Velocity Measurements in Open Channel Bores." *European Journal of Mechanics B/Fluids*, Vol. 32, pp. 52-58 (DOI 10.1016/j.euromechflu.2011.10.001) (ISSN 0997-7546).

Table 1 - Experimental studies of unsteady turbulence in tidal bores

Reference (1)	Q (m^3/s) (2)	B (m) (3)	S_o (4)	d_o (m) (5)	V_o (m/s) (6)	δ/d_o (7)	Fr (8)	Bed roughness (9)
Hornung et al.. (1995)	0	--	0	--	0	N/A	1.5 to 6	Smooth bed
Koch & Chanson (2008)	0.040	0.50	0	0.079	1.01	0.61	1.31 to 1.93	Smooth PVC
Present study								
Series 1	0.050	0.50	0	0.118	0.85	0.475	1.08 to 1.59	Smooth PVC
			0.002	0.125 ($^+$)	0.80	0.64	1.01 to 1.52	Fixed gravel bed (k_s = 3.4 mm)
Series 2	0.050	0.50	0.000	0.117	0.85	0.475	1.61	Smooth PVC
(ADV measurements)			0.002	0.126	0.79	0.64	1.50	Fixed gravel bed (k_s = 3.4 mm)

Notes: B: channel width; d_o: initial water depth at x = 5 m; Fr: tidal bore Froude number; k_s: equivalent sand roughness height; Q: initial flow rate; S_o: bed slope; V_o: initial flow velocity at x = 5 m; ($^+$): measured above the roughness.

Table 2 - Turbulent velocity processing techniques (used in the present study)

Processing technique (1)	Nb of experiments (2)	Basic processing (3)	Application (4)
Ensemble-average (EA) - median	20 repeats	ensemble-median	Laboratory
Variable interval time-average (VITA)	20 repeats	Filtering + ensemble-median	Laboratory
Variable interval time-average (VITA)	1 run	Filtering	Field data

CHANSON, H., and DOCHERTY, N.J. (2012). "Turbulent Velocity Measurements in Open Channel Bores." *European Journal of Mechanics B/Fluids*, Vol. 32, pp. 52-58 (DOI 10.1016/j.euromechflu.2011.10.001) (ISSN 0997-7546).

Fig. 1 - Breaking tidal bore of the Sélune River in Bay of Mont Saint Michel on 24 September 2010 - Bore propagation from right to left - Flow conditions: d_o = 0.37 m, U = 2 m/s, $(V_o + U) / \sqrt{g\,d_o}$ = 1.5

CHANSON, H., and DOCHERTY, N.J. (2012). "Turbulent Velocity Measurements in Open Channel Bores." *European Journal of Mechanics B/Fluids*, Vol. 32, pp. 52-58 (DOI 10.1016/j.euromechflu.2011.10.001) (ISSN 0997-7546).

Fig. 2 - Experimental channel

(A) Definition sketch

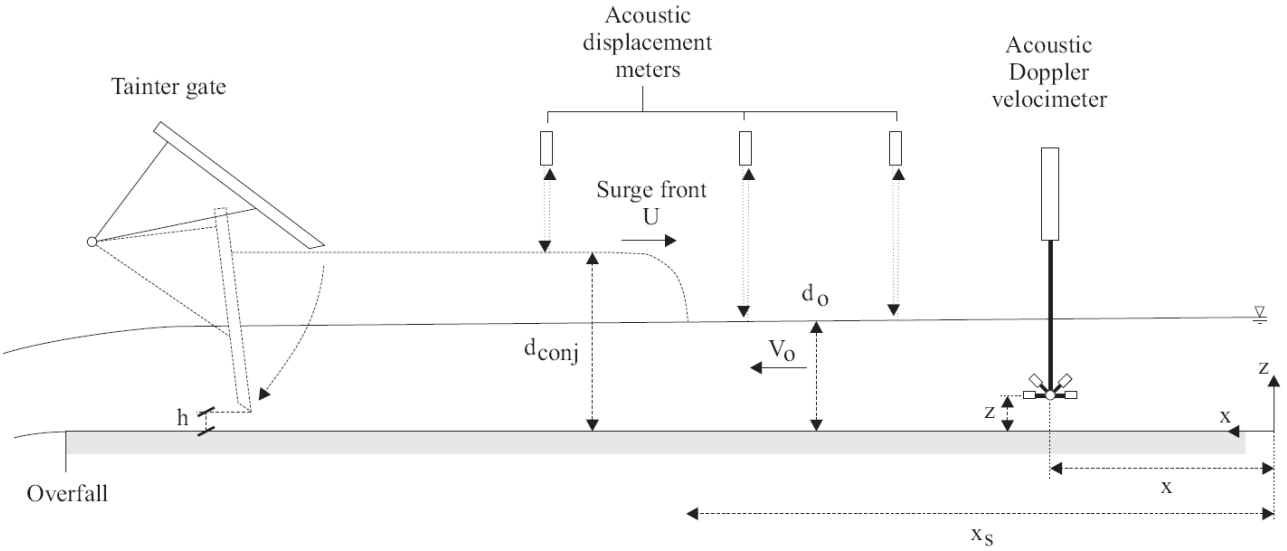

(B) Photograph of the flume with the gravel bed configuration, and the pointer gauge (left) and ADV head (right) above the free-surface

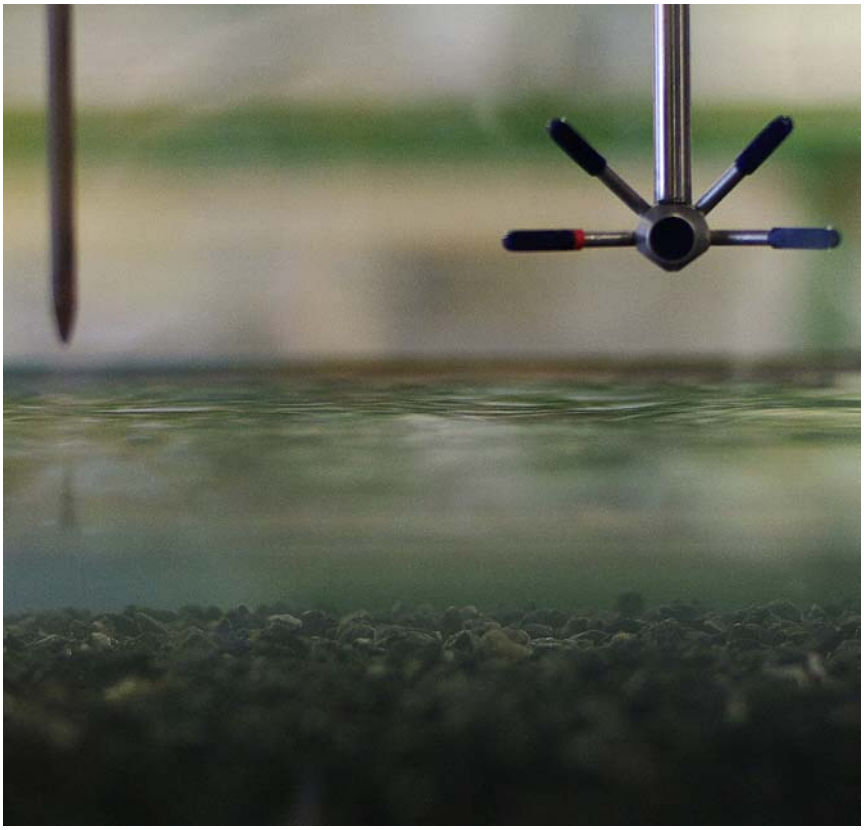

CHANSON, H., and DOCHERTY, N.J. (2012). "Turbulent Velocity Measurements in Open Channel Bores." *European Journal of Mechanics B/Fluids*, Vol. 32, pp. 52-58 (DOI 10.1016/j.euromechflu.2011.10.001) (ISSN 0997-7546).

Fig. 3 - Photographs of positive surges and bores

(A) Undular bore propagating from left to right - $Q = 0.050$ m^3/s, $d_o = 0.139$ m, Fr ≈ 1.1, h = 0.050 m, shutter speed: 1/50 s - The wave crest was at about x = 1 m

CHANSON, H., and DOCHERTY, N.J. (2012). "Turbulent Velocity Measurements in Open Channel Bores." *European Journal of Mechanics B/Fluids*, Vol. 32, pp. 52-58 (DOI 10.1016/j.euromechflu.2011.10.001) (ISSN 0997-7546).

(B) Looking downstream at the incoming breaking bore roller - Q = 0.050 m^3/s, d_o = 0.116 m, U = 0.85 m/s, Fr = 1.6, smooth PVC bed, high-speed photograph (shutter speed: 1/100 s)

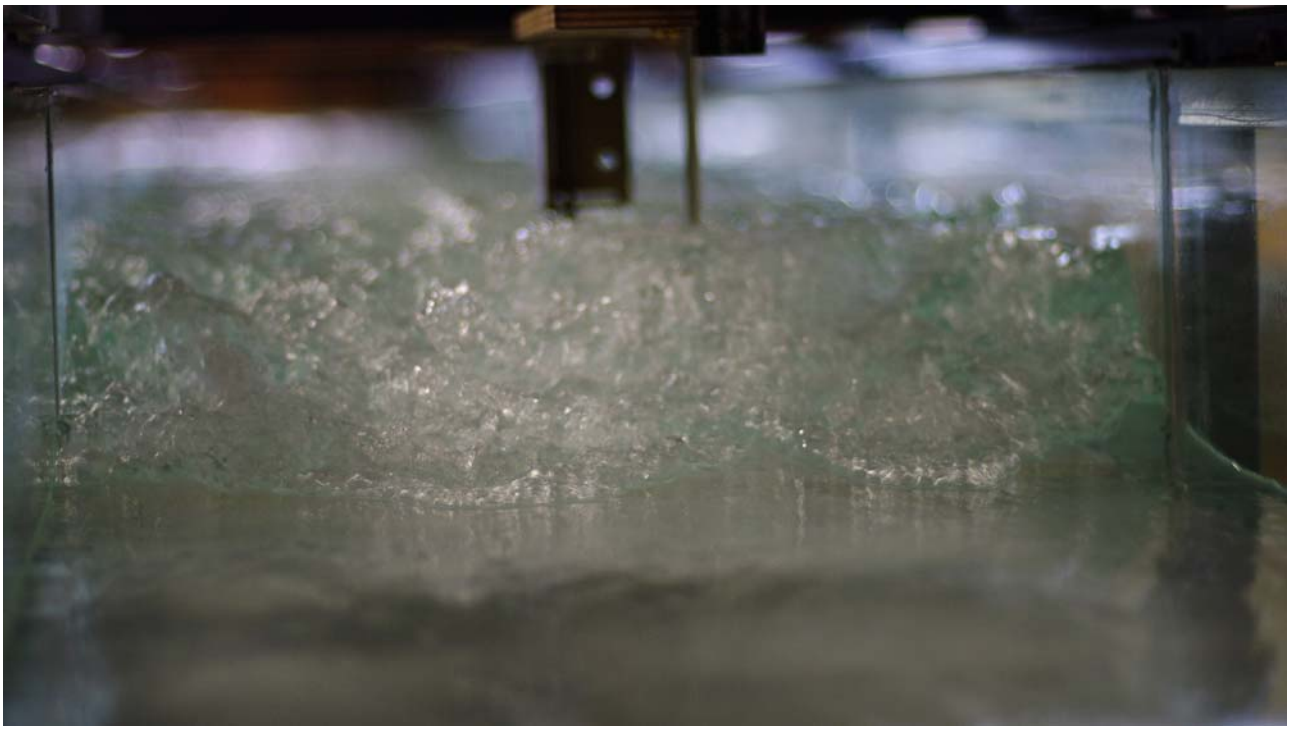

CHANSON, H., and DOCHERTY, N.J. (2012). "Turbulent Velocity Measurements in Open Channel Bores." *European Journal of Mechanics B/Fluids*, Vol. 32, pp. 52-58 (DOI 10.1016/j.euromechflu.2011.10.001) (ISSN 0997-7546).

Fig. 4 - Ratio of conjugate depths d_{conj}/d_o as a function of the bore Froude number - Comparison between the present data (Red symbols), earlier laboratory studies (Blue symbols: Favre 1935, Benet and Cunge 1971, Treske 1994, Koch and Chanson 2008), prototype data (Black symbols: Benet and Cunge 1971, Navarre 1995 [Dordogne River], Wolanski et al. 2004 [Daly River]), and the momentum equation (Eq. (2))

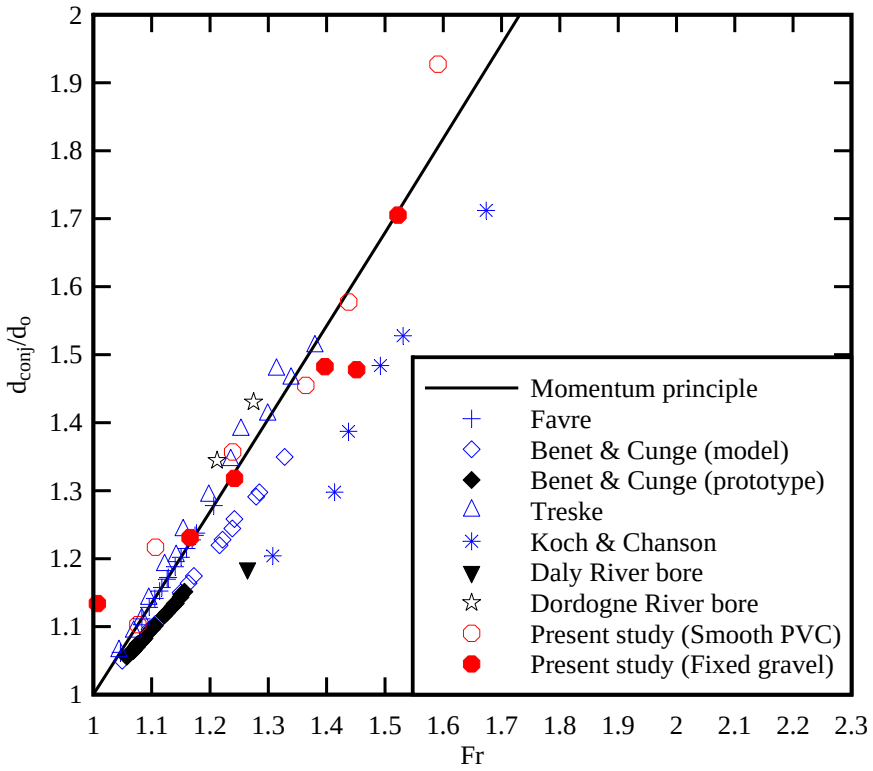

CHANSON, H., and DOCHERTY, N.J. (2012). "Turbulent Velocity Measurements in Open Channel Bores." *European Journal of Mechanics B/Fluids*, Vol. 32, pp. 52-58 (DOI 10.1016/j.euromechflu.2011.10.001) (ISSN 0997-7546).

Fig. 5 - Instantaneous free-surface elevation and turbulent velocities in a breaking bore on smooth PVC bed: Q = 0.050 m^3/s, d_o = 0.117 m, Fr = 1.6, ADV sampling volume elevation: z/d_o = 0.091

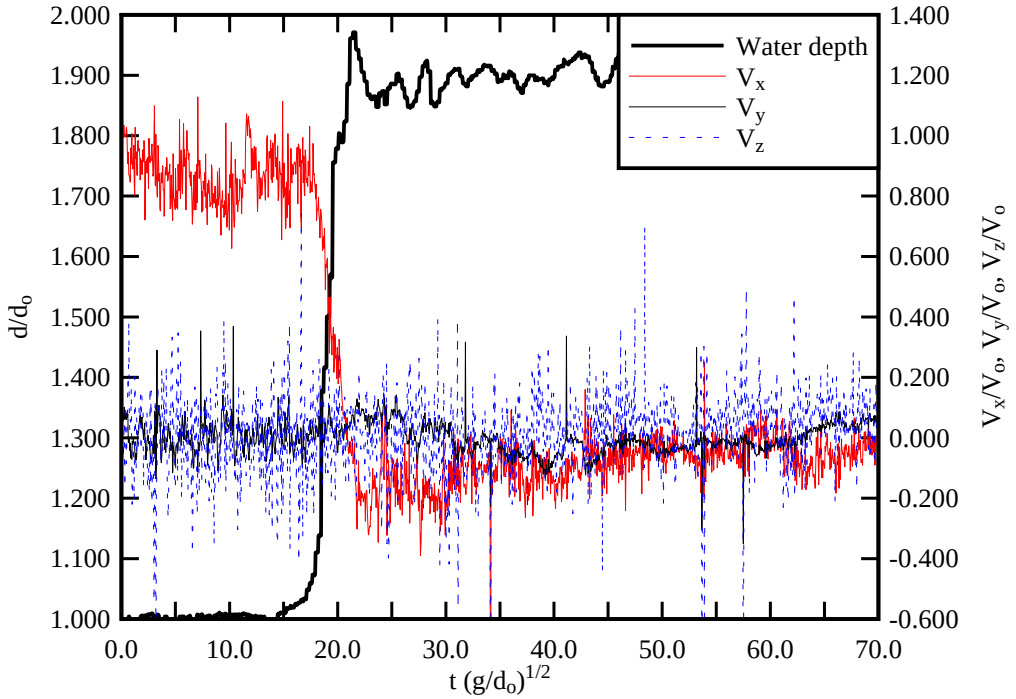

Fig. 6 - Sketch of the instantaneous free-surface measurement data during the breaking bore front passage

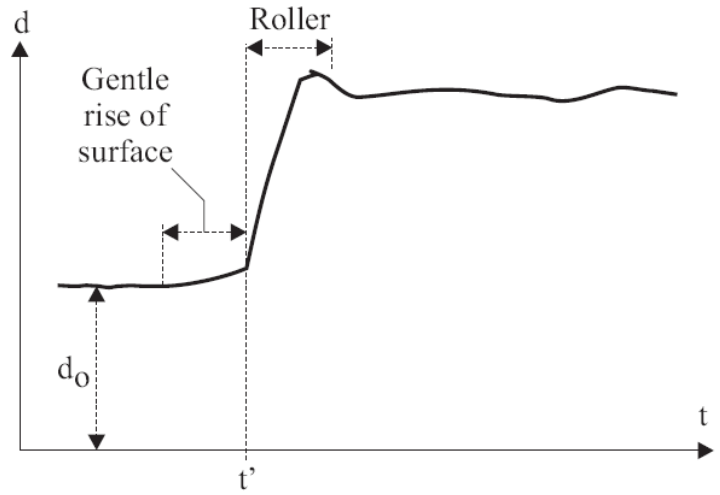

CHANSON, H., and DOCHERTY, N.J. (2012). "Turbulent Velocity Measurements in Open Channel Bores." *European Journal of Mechanics B/Fluids*, Vol. 32, pp. 52-58 (DOI 10.1016/j.euromechflu.2011.10.001) (ISSN 0997-7546).

Fig. 7 - Dimensionless ensemble-averaged median water depth d_{median}, ensemble-averaged median velocity component V_{median} (thick red dashed line), median value of the variable interval time average (VITA) velocity component (median value of 20 runs) (thick blue solid line), and low-pass filtered velocity components (VITA Runs 1 to 20) (thin black dotted lines) - Smooth PVC bed, Q = 0.050 m^3/s, d_o = 0.117 m, Fr = 1.6, ADV sampling volume elevation: z/d_o = 0.434

(A) Longitudinal velocity component V_x

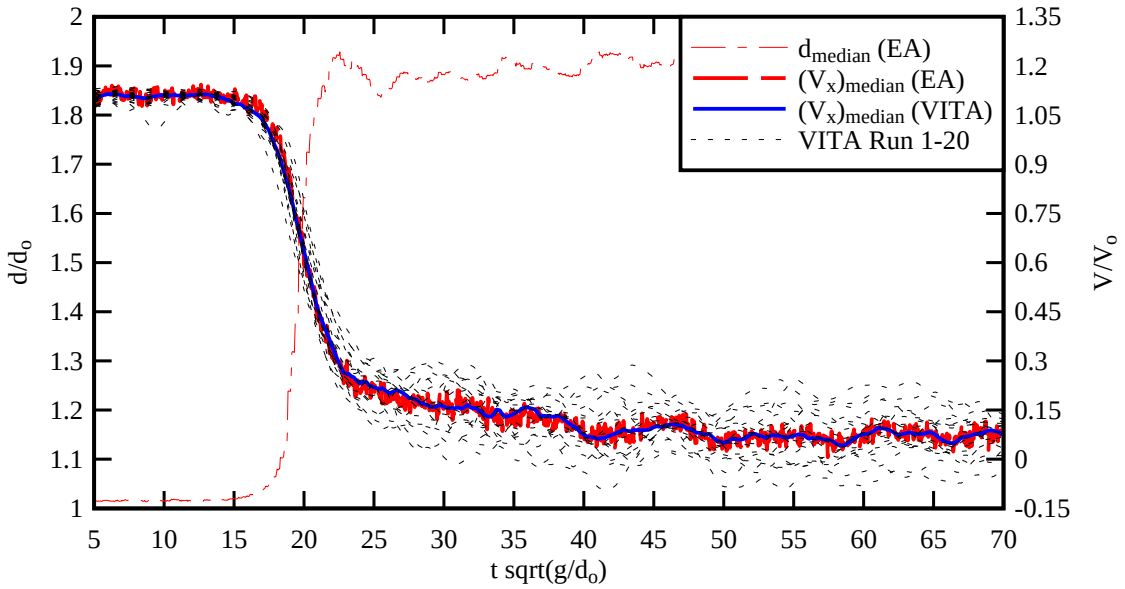

(B) Vertical velocity component V_z

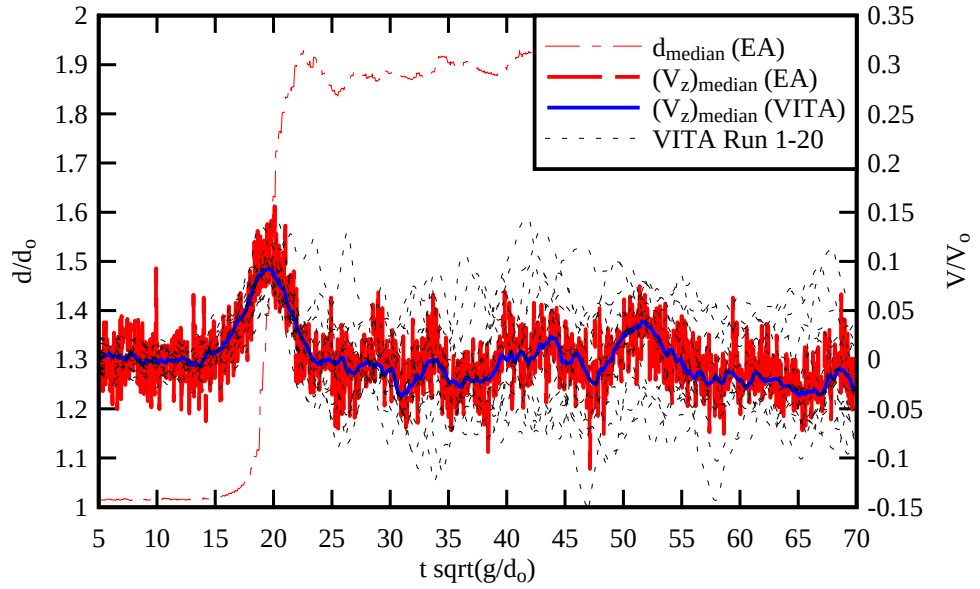

CHANSON, H., and DOCHERTY, N.J. (2012). "Turbulent Velocity Measurements in Open Channel Bores." *European Journal of Mechanics B/Fluids*, Vol. 32, pp. 52-58 (DOI 10.1016/j.euromechflu.2011.10.001) (ISSN 0997-7546).

Fig. 8 - Dimensionless ensemble-averaged median water depth d_{median} (thin red line), ensemble-averaged median longitudinal velocity component V_{median} (thick red dashed line), instantaneous data (Run 1, thin black line) and the low-pass filtered velocity component (VITA Run 1) (thick purple dashed line) - Fixed gravel bed, Q = 0.050 m^3/s, d_o = 0.126 m, Fr = 1.5, ADV sampling volume elevation: z/d_o = 0.131

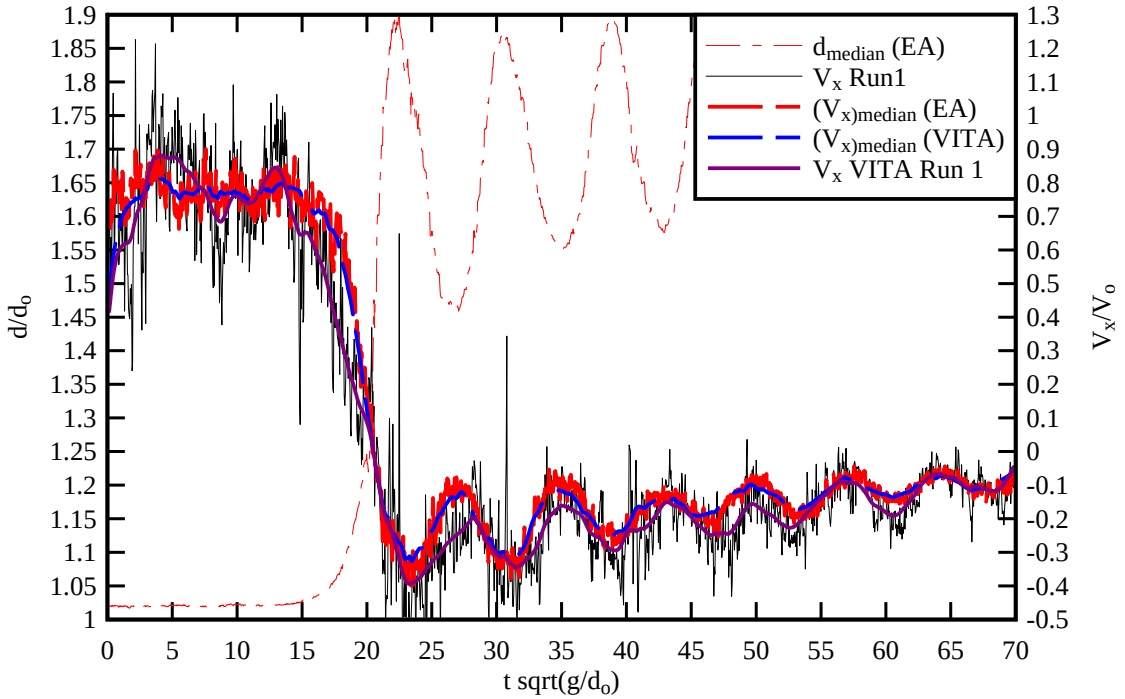

CHANSON, H., and DOCHERTY, N.J. (2012). "Turbulent Velocity Measurements in Open Channel Bores." *European Journal of Mechanics B/Fluids*, Vol. 32, pp. 52-58 (DOI 10.1016/j.euromechflu.2011.10.001) (ISSN 0997-7546).

Fig. 9 - Dimensionless ensemble-averaged median water depth d_{median}/d_o and median Reynolds stresses v_x^2/V_o^2 and $v_x \times v_y/V_o^2$ (Left), and v_y^2/V_o^2 and $v_y \times v_z/V_o^2$ (Right) on smooth PVC and fixed gravel beds - Comparison between ensemble-averaged and VITA calculations

(A) $z/d_o = 0.733$, Smooth PVC bed, v_x^2 & $v_x \times v_y$

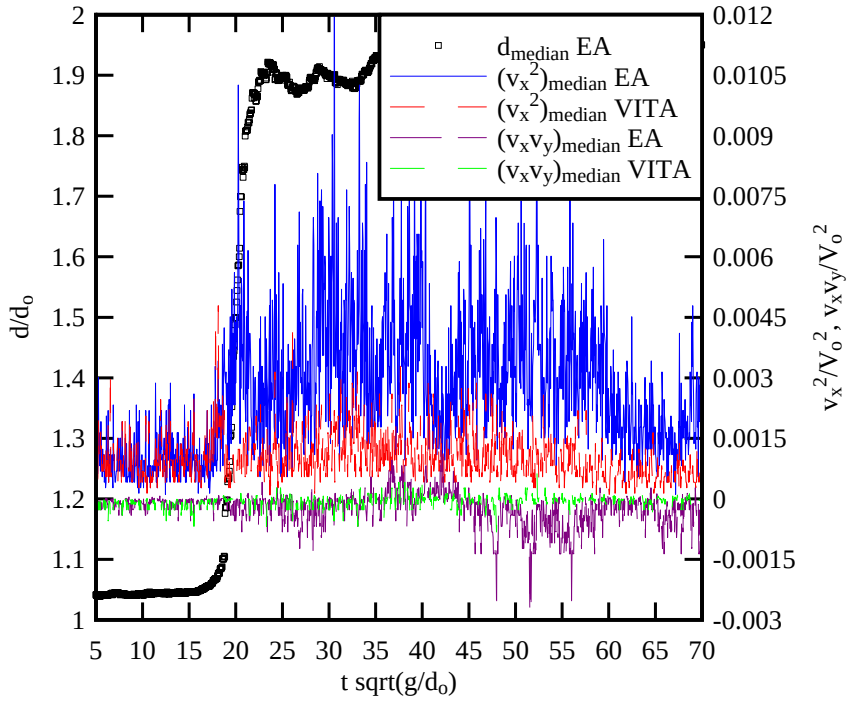

(B) $z/d_o = 0.733$, Smooth PVC bed, v_y^2 & $v_y \times v_z$

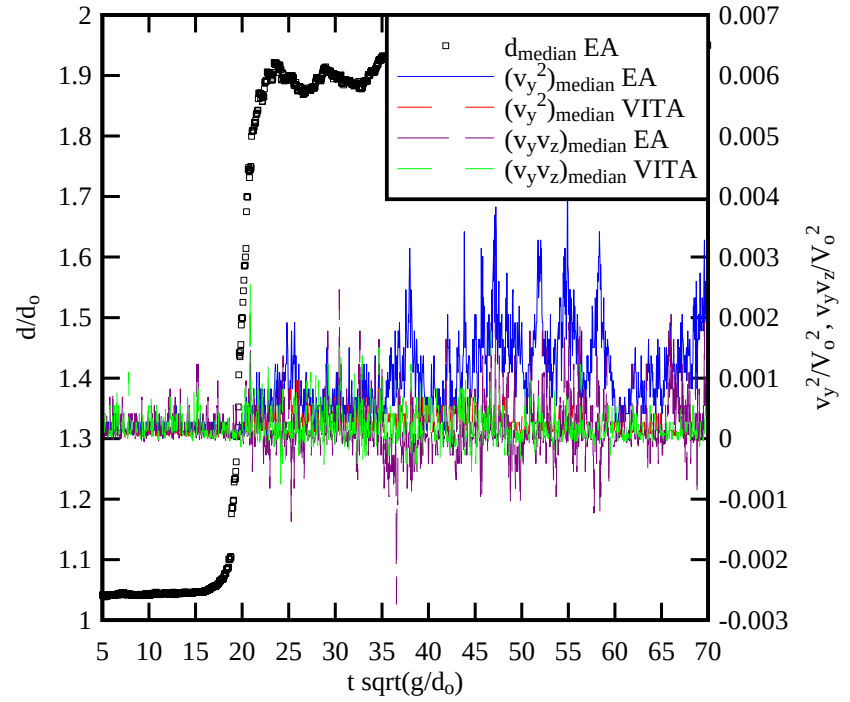

CHANSON, H., and DOCHERTY, N.J. (2012). "Turbulent Velocity Measurements in Open Channel Bores." *European Journal of Mechanics B/Fluids*, Vol. 32, pp. 52-58 (DOI 10.1016/j.euromechflu.2011.10.001) (ISSN 0997-7546).

(C) $z/d_o = 0.733$, Fixed gravel bed, v_x^2 & $v_x \times v_y$

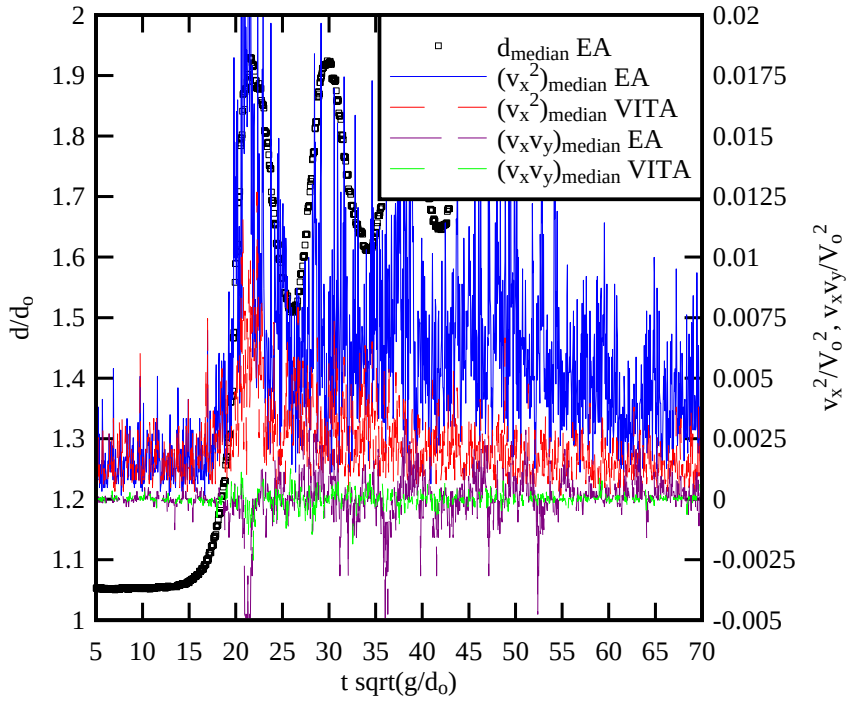

(D) $z/d_o = 0.733$, Fixed gravel bed, v_y^2 & $v_y \times v_z$